PNAS RESEARCH ARTICLE | NEUROSCIENCE

Distinct patterns of cortical manifold expansion and contraction underlie human sensorimotor adaptation

Daniel J. Gale[a], Corson N. Areshenkoff[a,b], Dominic I. Standage[a], Joseph Y. Nashed[a], Ross D. Markello[c], J. Randall Flanagan[a,b], Jonathan Smallwood[a,b], and Jason P. Gallivan[a,b,d,1]

Edited by Peter Strick, University of Pittsburgh Brain Institute, Pittsburgh, PA; received June 12, 2022; accepted October 17, 2022

Sensorimotor learning is a dynamic, systems-level process that involves the combined action of multiple neural systems distributed across the brain. Although much is known about the specialized cortical systems that support specific components of action (such as reaching), we know less about how cortical systems function in a coordinated manner to facilitate adaptive behavior. To address this gap, our study measured human brain activity using functional MRI (fMRI) while participants performed a classic sensorimotor adaptation task and used a manifold learning approach to describe how behavioral changes during adaptation relate to changes in the landscape of cortical activity. During early adaptation, areas in the parietal and premotor cortices exhibited significant contraction along the cortical manifold, which was associated with their increased covariance with regions in the higher-order association cortex, including both the default mode and fronto-parietal networks. By contrast, during Late adaptation, when visuomotor errors had been largely reduced, a significant expansion of the visual cortex along the cortical manifold was associated with its reduced covariance with the association cortex and its increased intraconnectivity. Lastly, individuals who learned more rapidly exhibited greater covariance between regions in the sensorimotor and association cortices during early adaptation. These findings are consistent with a view that sensorimotor adaptation depends on changes in the integration and segregation of neural activity across more specialized regions of the unimodal cortex with regions in the association cortex implicated in higher-order processes. More generally, they lend support to an emerging line of evidence implicating regions of the default mode network (DMN) in task-based performance.

sensorimotor learning | connectivity | cortical manifold | default-mode network | motor

Significance

We employed manifold learning techniques to understand how whole-brain cortical activity patterns reorganize when motor behavior must adapt to changing regularities in the environment. We found that important features of how we adapt our movements are reflected in changes in the relationship between regions of the association cortex, including areas of the default mode network, and unimodal systems more directly involved in visual and motor functions. We further show that the magnitude of this relationship is directly linked to how rapidly individuals learn. Together, our study establishes changes in the cortical landscape that emerge when we must adapt our behavior to changing environmental conditions and offers insights into the active role that the default mode network plays in task-based performance.

Adaptive behavior depends on aligning one's actions with the external constraints present in a given situation and updating this mapping in response to new demands (1, 2). Contemporary perspectives on brain function suggest that this process relies on cooperation between brain systems specialized for implementing behavior at the moment and those that help adapt behavior in the face of a changing environment. In the field of motor learning, much focus has been placed on identifying the contributions of several sensorimotor brain areas whose activity varies over the course of sensorimotor adaptation, a key form of learning by which the brain adjusts movement through trial-and-error (3–9). For instance, it is well understood that adaptation is supported, in part, by an implicit learning process wherein discrepancies between expected-versus-actual sensory outcomes (i.e., sensory prediction errors) are computed within the cerebellum (6, 8, 10, 11). These sensory prediction errors serve as a "teaching" signal to recalibrate subsequent motor commands in cortical sensorimotor regions, such as parietal, premotor, and motor cortices (12, 13) and thus gradually reduce errors over time.

In addition to this cerebellar-dependent learning process, emerging evidence indicates that sensorimotor adaptation is also supported by higher-order cognitive processing that takes place in the cortex (14–16). For instance, during sensorimotor adaptation, participants are able to use explicit knowledge about the change in environmental parameters in order to generate deliberate (and strategic) compensatory movements that minimize their movement errors (17–19). Along these lines, work has demonstrated that subjects who utilize this explicit knowledge are able to more rapidly reduce their errors during sensorimotor adaptation than participants who do not exhibit this same level of explicit knowledge (19–21). To date, neuroimaging and lesion studies have mainly implicated "task-positive" brain areas in the frontoparietal cortex, such as the dorsolateral prefrontal cortex (DLPFC) and inferior parietal cortex (15, 22, 23), as supporting the use of explicit strategies during sensorimotor adaptation. However, emerging perspectives on cortical organization highlight that even areas within the default mode network (DMN),

Author contributions: D.J.G., J.R.F., and J.P.G. designed research; D.J.G., D.I.S., and J.Y.N. performed research; D.J.G., C.N.A., and R.D.M. contributed new reagents/analytic tools; D.J.G. analyzed data; D.P.S. and J.Y.N. collected data; and D.J.G., J.S., and J.P.G. wrote the paper and secured funding for the work.

The authors declare no competing interest.

This article is a PNAS Direct Submission.

Copyright © 2022 the Author(s). Published by PNAS. This article is distributed under Creative Commons Attribution-NonCommercial-NoDerivatives License 4.0 (CC BY-NC-ND).

[1]To whom correspondence may be addressed. Email: gallivan@queensu.ca.

This article contains supporting information online at http://www.pnas.org/lookup/suppl/doi:10.1073/pnas.2209960119/-/DCSupplemental.

Published December 20, 2022.

which were initially viewed as "task negative" (24), may also be important when guiding task-related behaviors.

Positioned at the apex of cortical processing (25, 26), the DMN has been commonly attributed a role in mind-wandering, autobiographical memory, and internal mentation (24, 27–31). However, prior work has also implicated regions of the DMN, such as the medial frontal cortex and posterior cingulate cortex, as being involved in the exploration and implementation of strategies during task performance (32–34). This work is consistent with emerging perspectives of a role for the DMN in several aspects of task-based cognition, such as demanding working memory and decision-making tasks (35–38). Recent views argue that the broad contribution of the DMN to cognition, including during tasks, can be accounted for by its functional interactions with unimodal regions within sensory and motor networks (24, 39, 40). These interactions are thought to be enabled through its unique positioning on the cortical mantle, located equidistant between unimodal systems involved in perception and action, which is hypothesized to allow its broad oversight over brain-wide activity patterns (24, 26). Taken together, the recruitment of strategic processes during sensorimotor adaptation suggests that cortical regions in the association cortex, and possibly those located within the DMN, may play an important role in adapting motor behavior following a change in the environment.

Given that the association cortex is thought to exert influence on behavior through its topographical location on the cortex, in order to study the role of the DMN in cognition and behavior, it is necessary to use an analytic approach that explores cortical activity from a whole-brain connectivity perspective. In our study, therefore, we leverage advanced manifold learning approaches that provide a compact, low-dimensional description of changes in the overarching cortical functional architecture to explore and characterize the widespread involvement of the cortex during sensorimotor adaptation. Recent electrophysiological work has established that low-dimensional manifolds can provide a compact description of the covariance of neural population activity within regions of the premotor and motor cortices (41–43). At the same time, studies in other domains have applied the same logic to establish that low-dimensional representations of cortical activity can be a useful description of the macroscale organization of neural activity (44, 45). Recently, whole-brain manifolds, or gradients, have provided insight into the low-dimensional organization of brain structure and morphometry (46–48), intrinsic brain activity during rest (26), and changes in brain organization in clinical disorders (49–51) and throughout the lifespan (52–54). Here, we applied this approach to gain insight into how distributed cortical activity is coordinated during sensorimotor adaptation and how this changing cortical landscape unfolds across different phases of learning. Specifically, by estimating the relative positions of cortical brain regions in a connectivity-derived manifold space and understanding how these change in response to an environmental perturbation, we aimed to capture the evolving landscape of brain activity that supports sensorimotor adaptation as well as the features of this activity that relate to better or worse learning performance.

Results

We had participants ($N = 32$) perform a classic visuomotor rotation task (55) during functional MRI (fMRI) scans, in which they launched a cursor from an initial center position to a cued target that could be located in one of eight encircling positions on a visual display (Fig. 1*A*). Participants launched the cursor by applying a brief isometric directional force pulse on an MRI-compatible force sensor (*SI Appendix*, Fig. S1 for experimental setup). Following a Baseline block (120 trials), in which the cursor direction directly matched the force direction (Fig. 1 *A*, *Top*), the cursor was rotated 45° clockwise relative to the force direction for a remaining 320 trials (Fig. 1 *A*, *Bottom*). Overall, we found that participants' angular error was low during Baseline, indicating that individuals could perform the task with high accuracy (Fig. 1*B*). Following the onset of the rotation, errors increased significantly as participants had to learn how to counteract the cursor rotation to successfully hit each target (by aiming their hand in a 45° counterclockwise direction). Over time, participants were able to reduce their error to near-Baseline levels of performance, indicative of successful adaptation (Fig. 1*B*).

In order to study adaptation-related changes in functional cortical organization, we used three distinct, equal-length epochs over the time course of the task. Specifically, in addition to task Baseline (120 trials), we defined Early and Late adaptation epochs using the initial and final 120 trials, respectively, after rotation onset. Each epoch was treated as a continuous block of trials for estimating cortex-wide functional connectivity. For each participant, we extracted mean blood oxygenation level-dependent (BOLD) time series for each cortical region defined by the Schaefer 1000 parcellation (56) and estimated separate functional connectivity matrices for each epoch (Baseline, Early, and Late) using the covariance matrix of the time series (Fig. 1*C*). To reduce the influence of large individual differences in functional connectivity that can obscure any task-related changes (Fig. 1*D*; see also ref. 57), all connectivity matrices were centered according to a Riemannian manifold approach (*SI Appendix*, *Materials and Methods*; 58–60). Briefly, each participant's covariance matrices were translated to have a common mean (equal to the overall mean covariance) so as to remove static participant differences which may disguise task-related differences in functional connectivity. As the space of covariance matrices is non-Euclidean, this translation cannot be performed by ordinary subtraction but rather involves computing the difference between each covariance matrix and the corresponding participant mean (formally, a tangent vector) and then transporting this tangent vector to the overall grand mean in order to obtain a new covariance matrix which differs from the grand mean in an equivalent way. (See *SI Appendix*, *Materials and Methods* for the exact computations involved in this procedure.) To demonstrate the effect of this centering procedure—and its importance for elucidating learning-related effects in the data—we projected participants' individual covariance matrices, both before and after centering, using uniform manifold approximation (UMAP; 61). As can be seen in (Fig. 1 *D*, *Left*), prior to the centering procedure, functional network structure is dominated by participant-level clustering, which masks any task-related structure (i.e., differentiation of Baseline, Early, and Late learning). However, after centering (Fig. 1 *D*, *Right*), a task structure becomes more readily apparent.

To examine reconfigurations of cortical connectivity during visuomotor adaptation, we took the centered matrices and estimated separate cortical connectivity manifolds for each participant's Baseline, Early, and Late connectivity matrices. Using established procedures (26, 62, 63), each matrix was first transformed into an affinity matrix by computing the pairwise cosine similarity between regions after row-wise thresholding (*SI Appendix*, *Materials and Methods*). Then, we applied principal components analysis (PCA) to obtain a set of principal components (PCs), i.e., manifold, that provides a low-dimensional

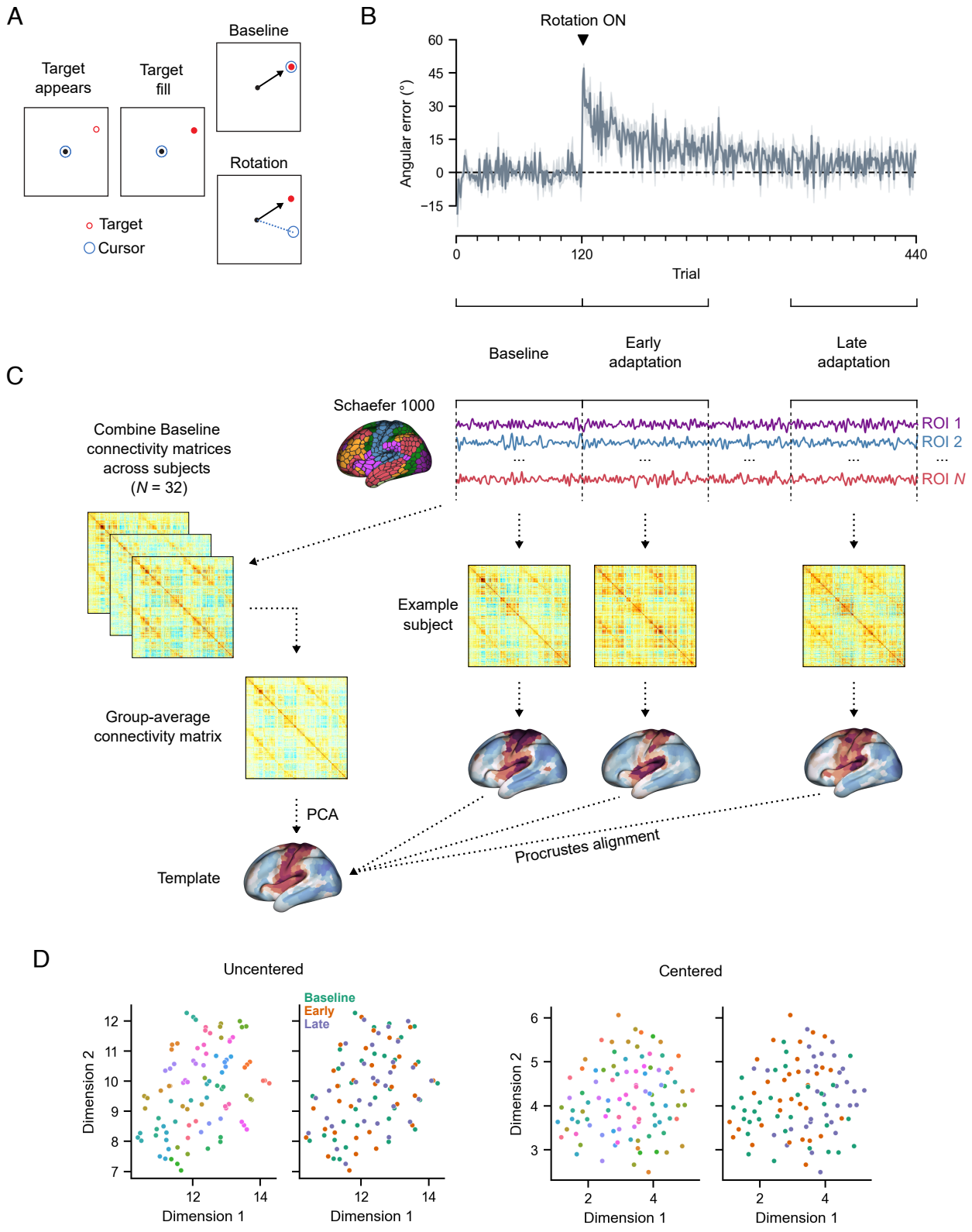

Fig. 1. Procedure and analysis overview. (*A*) Visuomotor rotation task. On Baseline trials, the cursor direction matched the aim direction. On rotation trials, the cursor direction was rotated 45° clockwise relative to the aim direction. (*B*) Average participant performance throughout the visuomotor rotation task. Shading indicates ±1 SEM. Three equal-length task epochs for subsequent neural analyses are indicated below: Baseline, Early adaptation (Early), and Late adaptation (Late). (*C*) Neural analysis approach. For each participant and each task epoch, functional connectivity matrices were computed using region-wise time series extracted with the Schaefer 1000 parcellation. Functional connectivity manifolds for each task epoch were estimated using PCA with centered and thresholded connectivity matrices (*SI Appendix, Materials and Methods*). All manifolds (participant × epochs) were aligned to a common template manifold created from a group-average Baseline connectivity matrix (*Left*) using Procrustes alignment. (*D*) Visualization of the similarity of connectivity matrices, both before and after centering, using UMAP. Note that uncentered connectivity matrices show strong participant-level clustering (*Outer-Left*, colored by participant), which masks differences in task structure (*Inner-Left*, colored by task). By contrast, centering removes this participant-level clustering (*Inner-Right*) and decouples task structure (*Outer-Right*) from these individual differences.

representation of cortical functional organization. Each matrix was then aligned to a template Baseline manifold, which was constructed using the mean of all Baseline connectivity matrices across participants (Fig. 1 *C*, *Right*). Crucially, not only did this template Baseline manifold provide a common target for manifold alignment (62) but it also allowed us to examine changes in cortical connectivity that selectively arise during the learning phase itself (i.e., Early and Late adaptation), thus increasing our sensitivity to detect deviations from the Baseline functional architecture.

Connectivity Manifold During Task Baseline. The top three PCs of the template Baseline manifold (Fig. 2*A*) provide a compact representation of the cortical functional organization during Baseline trials. PC 1 distinguishes somatomotor regions (positive loadings in red) from remaining cortical areas (negative loadings in blue), most prominently higher-order association regions within the DMN, such as posteromedial cortex (PMC), as well visual areas. Meanwhile, PC 2 illustrates a gradient between visual areas and the DMN, and PC3 is a joint gradient of i) superior-versus-inferior frontoparietal regions and ii) lateral-versus-medial occipital regions. These top three PCs collectively explain 49.30% of the total variance (Fig. 2*B*). Although only the top three PCs were retained for all subsequent analyses, we note that including PC 4, which explains nearly as much variance (8.98%) as PC 3 (9.63%), does not meaningfully alter our results and interpretations (*SI Appendix*, Fig. S2).

Mapping brain regions onto their assigned intrinsic functional network (56, 64) shows that PCs 1 and 2 jointly differentiate visual, DMN, and somatomotor regions, resembling the tripartite

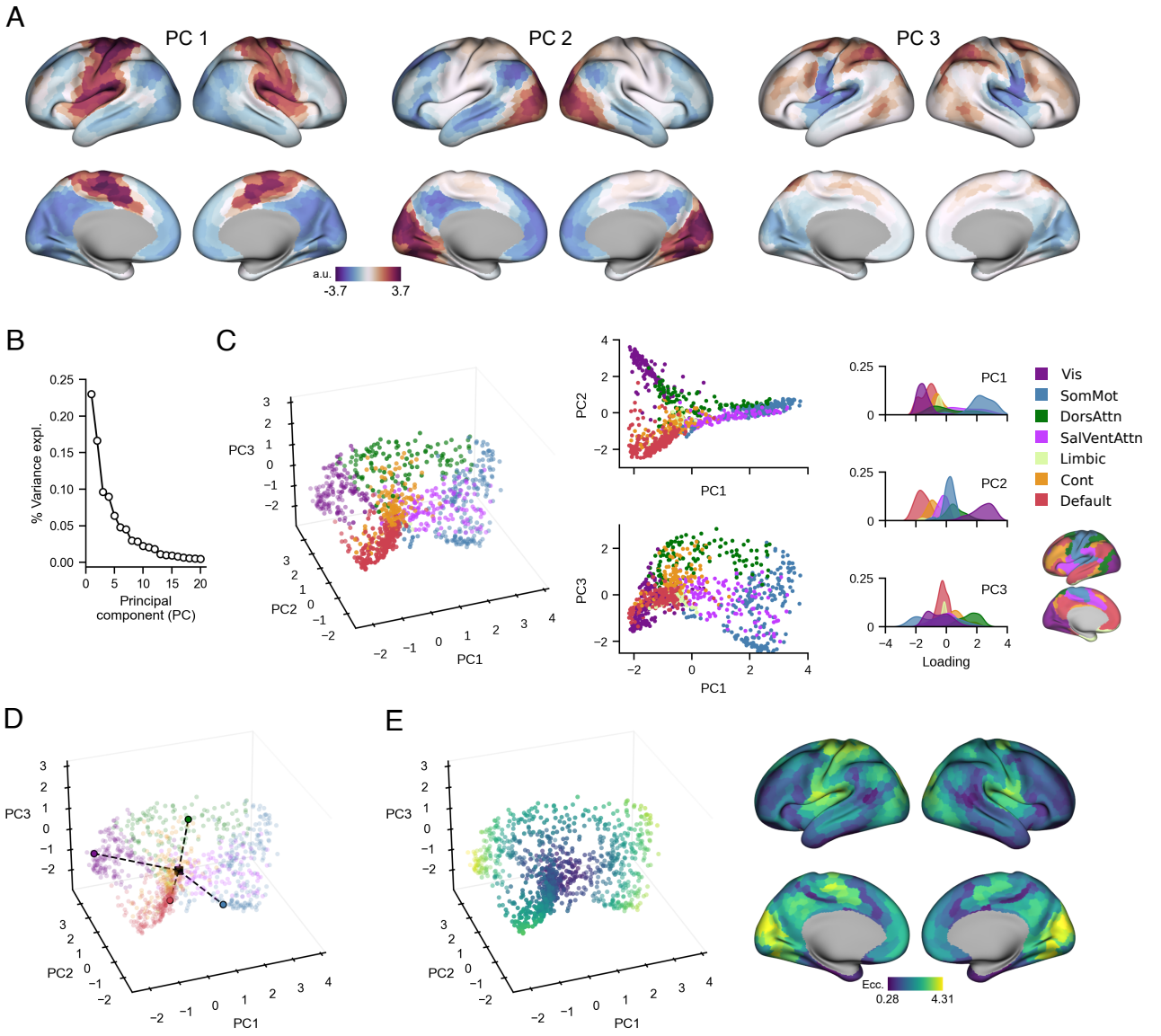

Fig. 2. Template Baseline manifold structure and eccentricity. (*A*) Region loadings for top three PCs of the template Baseline manifold (a.u.: Arbitrary units). (*B*) Percent variance explained for the first 20 PCs of the template Baseline manifold. (*C*) Functional network organization of the template Baseline manifold. *Right*, Scatter plots show the embedding of each region along the top three PCs, colored according to their intrinsic functional network (56, 64). *Left*, Probability density histograms show the distribution of each functional network along each PC. Vis: Visual. SomMot: Somatomotor. DorsAttn: Dorsal attention. SalVentAttn: Salience/Ventral attention. Cont: Control. (*D*) Visualization of the eccentricity calculation. Region eccentricity along the manifold is computed as the Euclidean distance (dashed line) from manifold centroid (black square). The eccentricity of four example brain regions is highlighted (bordered colored circles). (*E*) Regional eccentricity for the template Baseline manifold. Each brain region's eccentricity is color-coded and visualized in low-dimensional space (*Left*) and on the cortical surface (*Right*).

structure of resting-state connectivity gradients (Fig. 2*C*; 26). This differentiation is thought to reflect a fundamental feature of functional brain organization, in which the transition from the largely unimodal cortex (i.e., visual and somatomotor networks) to the transmodal cortex (i.e., DMN) represents a global processing hierarchy of increasing integration and abstraction from lower- to higher-order systems (25, 26, 65). In contrast, PC3 appears to be task-specific in that it isolates key dorsal attention, control, and somatomotor regions known to be involved in the planning and execution of hand movements required to successfully perform goal-directed actions, such as the dorsal premotor cortex (PMd), superior parietal cortex (SPC), and DLPFC (66–68).

Next, in order to characterize the relative positions of cortical brain regions along the Baseline connectivity-derived manifold space, which provides the basis for examining resultant changes in these positions throughout learning, we computed each region's manifold eccentricity by taking its Euclidean distance from the manifold centroid (Fig. 2*D*; 52, 53, 69). Eccentricity provides a multivariate index of each region's three-dimensional embedding, in which distal regions situated at the anchors of the manifold have greater eccentricity than proximal regions within the manifold core (Fig. 2 *E*, *Left*). Highly eccentric regions therefore can be interpreted as functionally segregated from other networks in the rest of the brain, as revealed by correlating eccentricity with graph theoretical measures of integration and segregation. We find that Baseline eccentricity is positively related to node strength ($r = 0.83$, two-tailed $P < 0.001$), defined as the sum of connectivity weights for a given region. Similarly, eccentricity is positively associated with the within-manifold degree z-score ($r = 0.49$, two-tailed $P < 0.001$), which indexes a region's connectivity within its own respective functional network. Together, these findings are consistent with the idea that eccentric regions are tightly interconnected with other members of the same functional network (*SI Appendix*, Fig. S3). Commensurate with this, eccentricity is negatively related to the participation coefficient ($r = -0.69$, two-tailed $P < 0.001$), which measures how evenly distributed the connections are across different functional networks. Therefore, eccentricity is inversely proportional to a region's degree of cross-network integration. Together, these results support the notion that adaptation-induced changes in a region's functional segregation or integration can be assessed through changes in eccentricity during Early and Late adaptation.

Manifold Reconfigurations During Adaptation. We found that the Early and Late adaptation epochs each exhibited distinct patterns of increases (i.e., expansion) and decreases (i.e., contraction) in manifold eccentricity relative to Baseline (Fig. 3*A*; for raw eccentricity maps, see *SI Appendix*, Fig. S4). To determine which regions showed significant changes in manifold eccentricity across the three task epochs (Baseline, Early, and Late adaptation), we performed region-wise repeated measures ANOVAs and corrected for multiple comparisons using false-discovery rate correction (FDR; $q < 0.05$). Across the cortex, we found that 131 regions showed a significant main effect of task epoch, i.e., adaptation-related changes, with 111 of these regions forming 14 contiguous clusters (Fig. 3*B*). Major clusters include contiguous regions spanning from the left (contralateral) PMd to SPC (18 regions), left PMC (20 regions), and dorsolateral portions of the bilateral extrastriate cortex (left = 22 regions; right = 11 regions). Smaller clusters and singleton regions were also observed throughout the rest of the cortex, and the combination of all clusters/regions spanned all six nonlimbic functional networks (Fig. 3*C*). Note that these topographical clusters arise because of the large degree of spatial autocorrelation along each dimension (see Fig. 2*A*). That is, topographically adjacent regions are more likely to have similar connectivity profiles and thus have similar projections onto the manifold.

To provide a concise summary of the ANOVA results presented above, we used k-means clustering to group regions with significant main effects according to their coordinates at Baseline (Fig. 3*C*, *colored circles*). This approach gave way to brain regions that tended to exhibit similar temporal trajectories in manifold space during adaptation (Fig. 3*C*, *traces*). The clustering analysis revealed four ensembles of regions (Fig. 3*D*): ensemble 1 (blue) is composed of somatomotor and dorsal attention network regions that load positively onto PC 1 and 3, which includes left sensorimotor regions that make up the largest cluster in Fig. 3*B*, along with right PMd and parietal regions; ensemble 2 (red) primarily involves higher-order transmodal areas of the DMN that load negatively onto PC 1 and 2, such as PMC, angular gyrus (AG), and superior temporal sulcus (STS); ensemble 3 (purple) mainly comprises visual regions, which include bilateral extrastriate and parahippocampal regions, which load negatively and positively onto PC 1 and 2, respectively; and ensemble 4 (yellow), which includes remaining regions in somatomotor and salience/ventral attention networks that load positively on PC1 but negatively on PC3. Computing the average eccentricity of each ensemble reveals distinct patterns of contractions and expansions along the manifold that characterize the key changes in connectivity during adaptation (Fig. 3 *D*, *Right*).

Next, we directly examined the region-based changes in eccentricity between each task epoch by performing follow-up paired t tests on the regions that exhibited significant main effects (in Fig. 3*B*), with corrections for multiple comparisons applied across all tests using FDR correction ($q < 0.05$; Fig. 3*E*). As revealed by a contrast of Early>Baseline, Early adaptation is primarily characterized by reductions in eccentricity, i.e., manifold contractions, of regions belonging to ensembles 1 and 2, including regions in the somatomotor and PMd, as well as areas of the DMN, such as bilateral PMC and AG. Although regions in ensemble 3 (visual network) collectively trend toward manifold contraction during Early learning (see Fig. 3*D*), only eight regions in extrastriate and parahippocampal cortices exhibited significant contractions, after corrections for multiple comparisons. Meanwhile, regions in ensemble 4 showed significant increases in eccentricity over the same time window, i.e., manifold expansion.

As revealed by the contrast of Late>Baseline (Fig. 3 *E*, *Middle*), we found that sensorimotor and DMN regions in ensembles 1 and 2, respectively, maintained their contraction during Late adaptation. Performing a Late>Early contrast (Fig. 3 *E*, *Bottom*) shows that the extent of the contraction in these regions did not significantly differ between epochs, with the exception of an increased contraction in the left somatosensory cortex and a subregion within the left PMC. However, by and large, the main characteristic feature of Late adaptation is the expansion of the visual cortex along the manifold, including bilateral extrastriatal regions. These effects are more pronounced for the Late>Early contrast than for the Late>Baseline contrast, which is a result of the overall trend toward manifold contraction of these visual areas during Early adaptation.

Taken together, the above pattern of results suggests that, during Early adaptation, several visual, sensorimotor, and transmodal areas in the DMN begin to integrate with regions outside of their

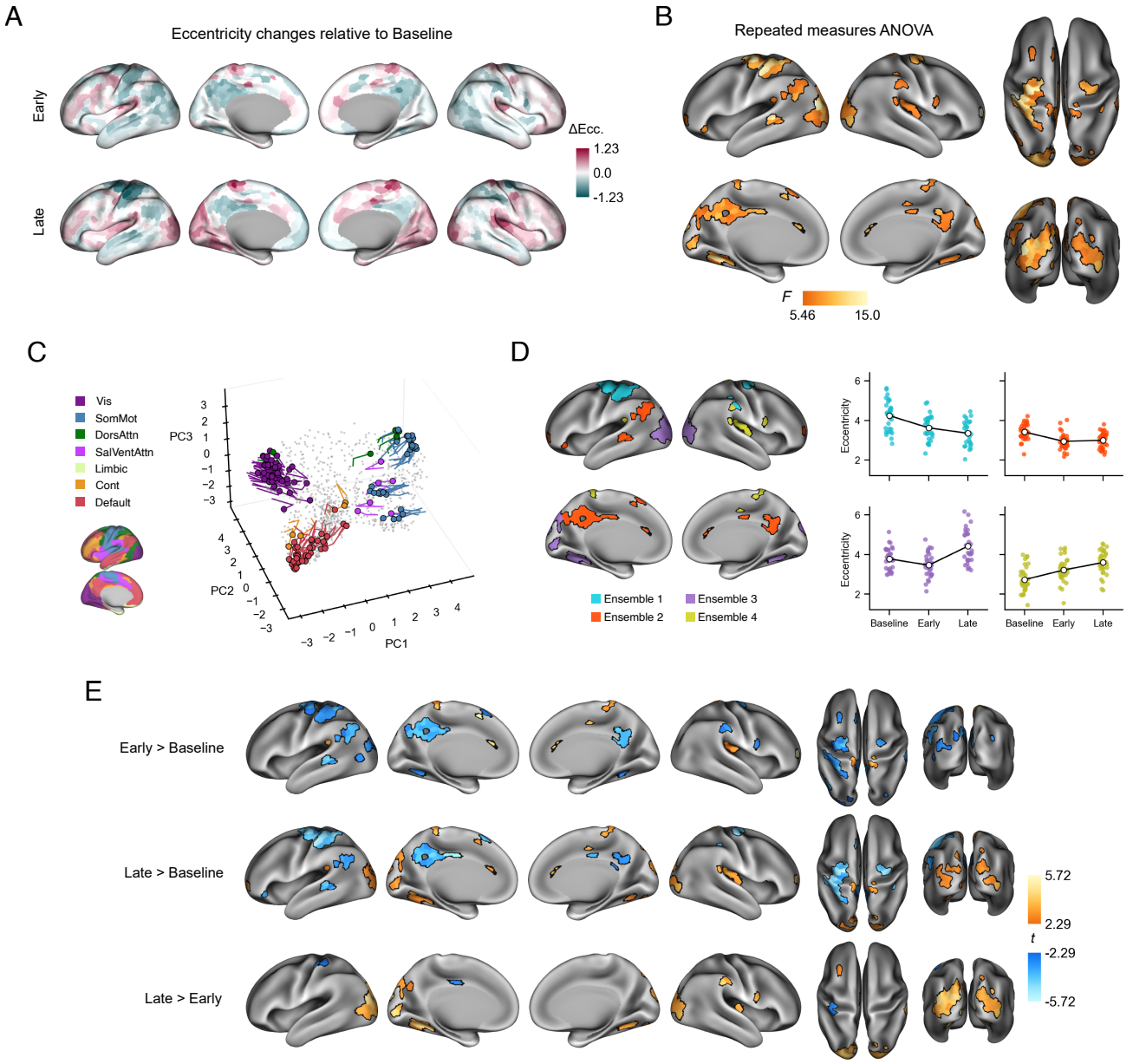

Fig. 3. Adaptation-related changes in manifold eccentricity. (*A*) Region-wise mean changes in eccentricity during Early and Late adaptation, relative to Baseline. Positive (mauve) and negative (teal) values indicate relative increases and decreases in eccentricity, respectively. (*B*) Significant changes in eccentricity across task epochs (Baseline, Early, and Late) according to region-wise repeated measures ANOVAs with false-discovery rate (FDR) correction for multiple comparisons ($q < 0.05$). (*C*) Temporal trajectories of statistically significant regions from *B* in low-dimensional space. Colored circles indicate each region's initial position during Baseline, and the traces show the unfolding displacement of that region during Early and Late adaptation. Each region is colored according to its functional network assignment (*Left*). Nonsignificant regions are shown in gray point cloud. (*D*) Patterns of effects for four ensembles of significant regions in *B* derived from *k*-means clustering on each brain region's coordinates during Baseline (see *C*). Scatter plots (*Right*) show within-ensemble mean eccentricity for each participant, and line plot overlays (white markers) show the group mean across task epochs. (*E*) Pairwise contrasts of eccentricity between task epochs. Region-wise paired *t*-tests were performed for each contrast, and FDR correction was applied across all comparisons ($q < 0.05$). Positive (orange) and negative (blue) values show significant increases and decreases in eccentricity, respectively.

respective functional networks. By contrast, during Late adaptation when performance plateaus and errors become minimized, our findings suggest that visual cortical regions, particularly higher-order visual areas, become functionally segregated from other brain networks. In the next section, we seek to directly test these interpretations of manifold contractions and expansions during Early and Late adaptation, respectively.

Connectivity Changes Underlying Manifold Reconfigurations. Because eccentricity represents a multivariate measure of a region's overall connectivity profile, we performed seed connectivity analyses in order to help characterize the changes in connectivity that underlie the patterns of manifold contraction and expansion we observed throughout adaptation. To describe connectivity changes during Early adaptation, we selected representative regions of the three largest clusters in the Early>Baseline contrast, which included the left PMC, left SPC, and left PMd (*SI Appendix, Materials and Methods*). For each region, we contrasted seed connectivity maps between the Early and Baseline epochs (Early>Baseline) by computing region-wise paired *t*-tests, producing contrast maps for each seed region (Fig. 4*A*). We show the unthresholded contrast maps to allow visualization of

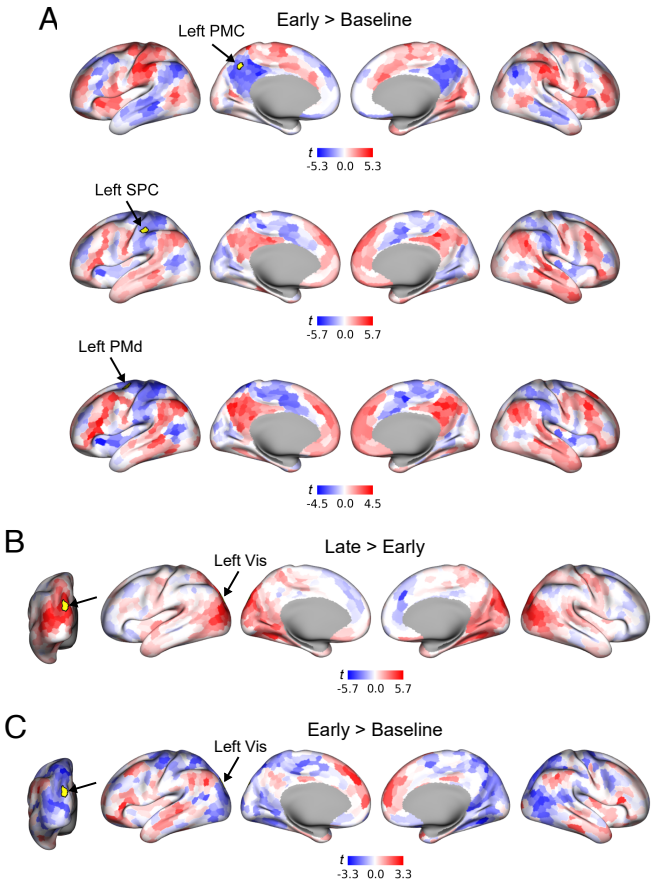

Fig. 4. Patterns of connectivity differences underlying changes in manifold eccentricity. (*A*) Early>Baseline seed connectivity contrast maps for the left PMC, SPC, and PMd. Selected seed regions are shown in yellow and are also indicated by arrows. Positive (red) and negative (blue) values show increases and decreases in connectivity, respectively, during Early adaptation relative to Baseline. (*B*) Late>Early and (*C*) Early>Baseline seed connectivity contrast maps for the left visual/extrastriate (Vis) seed region.

the complete array of connectivity differences that collectively contribute to the eccentricity changes.

During Early adaptation, we found that the left PMC seed region exhibited decreased connectivity with other PMC subregions across both hemispheres as well as with other DMN areas located in bilateral AG and STS and with the left DLPFC. Instead, the PMC exhibited increased connectivity with sensorimotor regions such as the PMd and SPC, along with anterior portions of the frontal cortex and insula. Notably, the opposite pattern can be observed for both the left SPC and PMd seed regions, which exhibited decreased connectivity with other sensorimotor regions in favor of increasing their connectivity with areas of the DMN (e.g., bilateral PMC, AG, STS) and the DLPFC. Together, these findings indicate that manifold contractions of the PMC, SPC, and PMd during Early adaptation largely arise from increased integration between sensorimotor regions (ensemble 1) and higher-order transmodal regions of the DMN (ensemble 2).

We also repeated the seed connectivity analysis to investigate the basis of the manifold expansion of the visual cortex observed during Late adaptation. Using the Late>Early eccentricity contrast, we selected a representative region from the left extrastriate cluster, which was the largest cluster across both hemispheres. By contrasting seed maps between the Late and Early epochs (i.e., Late>Early), we found that connectivity increased within bilateral visual cortex and parahippocampal regions (Fig. 4*B*). Meanwhile, connectivity to the rest of the cortex remained relatively unchanged, with the exception of subtle connectivity reductions in the dorsomedial frontal cortex. These results suggest that the segregation/expansion of visual areas during Late adaptation is mainly driven by increased intraconnectivity of the visual cortex rather than a decoupling from the rest of the cortex. Notably, this same visual seed region also exhibited a significant contraction in our Early>Baseline eccentricity contrast (see Fig. 3*E*), and as such, we additionally contrasted this region's seed connectivity during the Early and Baseline epochs. This analysis revealed decreased connectivity with visual and sensorimotor regions during Early adaptation, while also showing increased connectivity with DMN areas, such as AG, STS, and dorsomedial frontal cortex (Fig. 4*C*). Thus, consistent with the pattern of effects shown above for areas PMC, SPC, and PMd, we found that greater connectivity with the DMN also underlies significant manifold contractions of visual areas. Together, this suggests that increased functional interaction between unimodal and transmodal cortical areas is a feature of early learning.

Eccentricity Relates to Performance During Early Adaptation. Thus far, we have characterized within-participant alterations to manifold structure throughout adaptation, revealing patterns of manifold contraction and expansion expressed across individuals. It is well established, however, that significant intersubject variability exists during the initial phases of learning, when visumotor errors are largest (17–19). Consistent with this prior work, we find a large degree of between-participant variability in performance during Early adaptation (Fig. 5*A*), which we measured by computing the median angular error for each participant (i.e., Early error; Fig. 5*B*). Given these prominent individual differences in performance, we next asked whether this intersubject variability is related to manifold structure during Early adaptation, as captured by eccentricity.

To examine this question at the region level, we calculated the correlation between participants' Early error and the eccentricity values within each cortical region during Early adaptation (Fig. 5*C*). Following FDR correction for multiple comparisons ($q < 0.05$), we found that regions within the left (contralateral) parietal cortex and bilateral PMd exhibited significant positive associations between their manifold eccentricity and participant Early error (i.e., greater eccentricity corresponds with a greater error or worse performance). Note that, across participants, these same regions exhibit overall manifold contractions during Early adaptation (see Fig. 3*E*), and thus, participants with greater contractions (i.e., lower eccentricity) in these regions during Early adaptation show faster learning (i.e., lower Early error). Also, recall that manifold contractions of these same regions (the left PMd and SPC seed regions used for connectivity analyses Fig. 5*C*, *arrows*) are associated with increased connectivity with higher-order transmodal regions within the DMN (Fig. 4*A*). Taken together, these findings suggest that participants who adapt more rapidly express a greater degree of integration between sensorimotor and higher-order association networks during Early adaptation. This is consistent with the idea that the coupling of transmodal and sensorimotor cortical regions during adaptation reflects the recruitment of explicit learning processes, which exert top–down control over the sensorimotor system (16–18).

It is noteworthy that the region-level correlations shown in Fig. 5*C* exhibit a high degree of spatial contiguity; that is, the

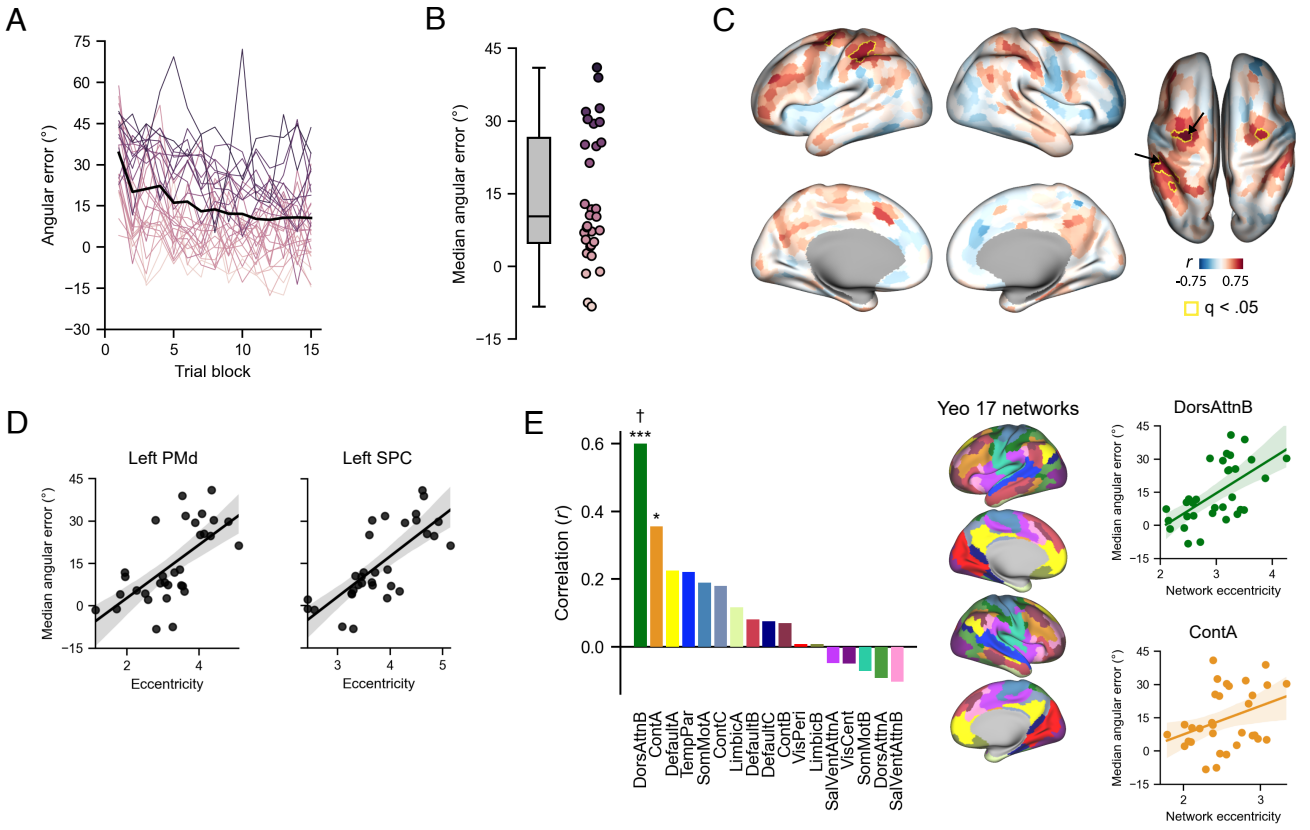

Fig. 5. Manifold eccentricity during Early adaptation relates to task performance. (*A*) Individual differences in behavioral performance during Early adaptation. The black line shows the average error across participants, binned by trial block, and colored traces show binned error for individual participants. Different participants are colored according to their median error in *B*. (*B*) Distribution of median error during Early adaptation. Color in the scatter plot indicates median error, with lighter color in the scatter plot indicating a lower Early error (better learning). (*C*) Correlation map between Early eccentricity and Early error. Yellow traces show significant regions following FDR correction ($q < 0.05$). Arrows indicate left PMd and SPC seed regions in Fig. 4*A*, which are used as exemplar significant regions in *D*. (*D*) Example correlations from left PMd and SPC seed regions in Fig. 4*A*. (*E*) Correlations between network eccentricity and Early error (*Left*); scatter plots are shown for the two largest correlations (*Right*). Bar and scatter plot colors correspond to network colors shown on the brain surface (*Middle*). Of all networks, Dorsal Attention B and Control A showed the strongest correlations (*Right*). VisCent: Visual Central. VisPer: Visual Peripheral. SomMotA: Somatomotor A. SomMotB: Somatomotor B. TempPar: Temporal Parietal. DorsAttnA: Dorsal Attention A. DorsAttnB: Dorsal Attention B. SalVentAttnA: Salience/Ventral Attention A. SalVentAttnB: Salience/Ventral Attention B. ContA: Control A. ContB: Control B. ContC: Control C. $^{*}P < 0.05$, $^{***}P < 0.001$, $^{\dagger}q < 0.05$.

parietal and premotor cortical regions that pass FDR correction (noted above) are situated within much larger clusters of regions that exhibit a very similar pattern of correlations with learning performance. This topography suggests that the association between manifold eccentricity and participant behavior during Early adaptation may be further characterized at the level of distributed functional networks. To explore this possibility, we mapped each region onto its respective functional network and, within each participant, computed the average manifold eccentricity for each network (i.e., network eccentricity). For this purpose, we used the 17-network mapping in order to capitalize on the improved spatial precision—and thus the ability to better localize effects—compared to the 7-network mapping (56, 64). Next, we correlated, for each network, its eccentricity during Early adaptation with participants' Early error. Among these networks, the Dorsal Attention B ($r = 0.60$, two-tailed $P < 0.001$; Fig. 5*E*) and Control A ($r = 0.35$, two-tailed $P = 0.046$) networks showed a significant positive association with Early error (although the Control A did not survive FDR correction, $q < 0.05$). Collectively, these two networks span several parietal (e.g., SPC, intraparietal sulcus), premotor (e.g., PMd, frontal eye fields), and prefrontal areas (e.g., DLPFC), which together represent an array of brain areas previously implicated in higher-order sensorimotor processing and the top–down control of goal-directed behavior (67, 70–72).

Discussion

Complex behavior depends on the coordinated operation of several specialized neural systems distributed throughout the brain. During sensorimotor adaptation, these distributed systems must modify their interactions to ensure that motor behavior appropriately responds to changes in environmental dynamics and regularities. While much focus to date has been on understanding the cerebellar-dependent mechanisms that underlie sensorimotor adaptation, our understanding of the contributions and functional reorganization of cortical systems remains incomplete (73). Here, we capitalized on recent analytical methods that link together topographic and functional brain organization (26, 62) in order to quantify adaptation-related changes in cortical activity patterns and how features of this reorganization relate to learning performance.

By projecting subjects' cortical functional connectivity patterns into compact low-dimensional manifold spaces, we found that adaptation was primarily characterized by increasing manifold contractions of higher-order sensorimotor regions in the parietal and PMd cortex, as well as transmodal areas of the DMN.

Further analyses revealed that these manifold contractions were the result of greater covariance in neural activity between transmodal (i.e., DMN and frontoparietal networks) and unimodal (i.e., sensorimotor) systems, which was largely maintained across the entire adaptation period. In addition, we found that, by the late stages of adaptation, when visumotor errors had been largely reduced, visual cortical regions exhibited expansion along the cortical manifold, a pattern that was explained by greater intraconnectivity within the visual cortex. Finally, our analyses revealed that these changes have important behavioral correlates, as faster overall adaptation was linked to increased covariance between sensorimotor and transmodal areas of the DMN. Together, our results characterize the macroscale cortical changes that support human sensorimotor adaptation and performance. As we discuss below, these findings have important implications for our understanding of the cortical basis of adaptation, in general, and the role that the association cortex, and the DMN, in particular, plays in the organization of adaptive behavior.

Several prior fMRI studies have revealed adaptation-related increases and decreases in the activity of individual sensorimotor cortical brain regions, including areas in the motor, premotor, and parietal cortex (3–5, 7, 22, 74). Our results expand on these findings by suggesting that these individual region-based changes are part of a broader reorganization of the cortical landscape that occurs during adaptation. Specifically, our analyses suggest that sensorimotor areas become increasingly integrated with higher-order association areas in the DMN and DLPFC following a visuomotor perturbation. Contemporary models of cortical organization (25, 26) suggest that transmodal regions are important for organizing behavior in an increasingly abstract manner. It is possible that the observed changes in the cortical landscape, therefore, reflect the increased need for more abstract control over unimodal systems. This perspective is consistent with behavioral and lesion work indicating that adaptation recruits cortically driven explicit learning processes (e.g., mental rotation, working memory, etc.) that are strategic and declarative in nature and thus presumed to involve brain areas in the higher-order association cortex (e.g., prefrontal regions; 15, 23). Furthermore, existing evidence suggests that faster learning across participants results from the greater recruitment of explicit learning processes during adaptation (19). Consistent with this, we find that faster learning across participants is associated with a greater manifold contraction of higher-order sensorimotor regions in the parietal and PMd cortex and that these contractions reflect the increased covariance of these areas with regions of the DMN and prefrontal cortex (Fig. 4). We find it noteworthy that these parietal and premotor cortical areas belong to the dorsal attention (DAN) network (see Fig. 5*E*), given that this network, in particular, has been heavily implicated in the top–down control of attention and action (64, 70, 72). However, we recognize that, although our study highlights the interactions of both unimodal and transmodal systems during learning, our design does not allow us to delineate the specific higher-order control processes that this pattern reflects. For instance, the extent to which these interactions may be linked to task-general processes, such as changes in cognitive effort (75), attention (76), or inhibition (77), which all play critical roles in shaping learning (78–80), remains a question for future work.

Our data also have important implications for understanding how and under what conditions the DMN contributes to ongoing behavior. Initial observations that the DMN was often less active in external tasks led many researchers to focus solely on processes that are likely to occur in this context. These included introspective states such as mind-wandering (28) or mental time travel (30, 81) as well as aspects of both episodic (30) and semantic memory (82). However, while the DMN is undoubtedly important in these situations, recent research highlights the need to go beyond these cognitive domains for two different reasons. First, contemporary observations from cognitive neuroscience suggest that even during complex demanding external tasks, the DMN systematically changes its functional organization in a manner that reflects features of the external task. For example, in working memory (39) and feature discrimination paradigms, (83) regions of the DMN can increase connectivity with task-positive regions, such as the DLPFC, in a manner that is linked to better performance. In externally demanding situations, experience sampling studies highlight that regions, such as the posterior cingulate cortex, are important for supporting patterns of detailed task-relevant cognition (35, 40). Moreover, in externally demanding tasks, in which memory is important for guiding decisions, activity levels within the DMN can increase even if the task stimuli are simple geometric shapes and thus lack complex semantic or episodic associations (36–38). Second, contemporary anatomical perspectives on the DMN have demonstrated that it is situated at the apex of processing streams originating in the sensorimotor cortex, a location that highlights its potential role in the governance of integrated forms of behavior (24, 26). In the context of the current work, our study shows that greater functional integration between the DMN and sensorimotor systems can occur when simple visumotor regularities that govern reaching behavior change and that this integration has functional significance in terms of how rapidly behavior can be adapted. In this way, our study extends the situations in which the DMN contributes to cognition and behavior beyond the domain of purely "cognitive" tasks to tasks involving visumotor control.

We envisage two ways in which the DMN may contribute to sensorimotor learning. First, the DMN may support a memory of past visumotor errors (84) experienced by the participant, which is used as a basis for guiding learning. Indeed, prior work has shown the DMN to be involved in situations where decision-making cannot be based on immediate sensory input and must instead be guided by prior information (e.g., from a previous trial) (35–39, 85). By analogy, in error-based sensorimotor learning, action selection on the current trial (i.e., what direction to move) is based on a recent history of errors accrued across previous trials (84). It is possible that this memory process is supported by the DMN, which then communicates with the sensorimotor system to update future motor actions accordingly. A second way in which the DMN may contribute to sensorimotor learning is the search for, and implementation of, a reaiming strategy during learning (18, 86). For example, the DMN may be involved in exploration of a correct reaiming strategy during initial learning, whereas during later learning, the DMN is involved in remembering and implementing that learned strategy (32, 34). From this perspective, the link between the reconfiguration of functional relationships between the DMN and sensorimotor cortices, as well as their relationships to behavioral performance, may reflect the neural motif through which we explicitly consider and modify our actions. Understanding how we flexibly control our actions based on current goals and prior knowledge about the environment is an important question for future work, as it will help identify whether the patterns of neural effects observed here are unique to situations of sensorimotor adaptation or, instead, reflective of a more general process for controlling real-time behavior.

One curious observation was our finding that the visual cortex exhibited contraction along the cortical manifold during Early adaptation, whereas during Late adaptation, it exhibited expansion (Fig. 3*E*). Our further analyses indicated that this reversal pattern resulted from the relative increase in covariance, during Early adaptation, between the visual cortex and areas of the DMN (e.g., medial prefrontal cortex, AG, superior temporal gyrus) compared to a relative decrease in this covariance during Late adaptation. While we can only speculate on the nature of these changes, one possibility is that they reflect a relative shift in the neural processing of visual errors experienced by participants across the different phases of learning. During Early adaptation, subjects experience large visual errors (~45°), which tend to engage explicit reaiming processes to help minimize those errors (87). At the neural level, this would require that errors sensed by the visual system be fed forward to the higher-order association cortex, which, in turn, would implement a reaiming strategy to help reduce those visual errors. This would presumably manifest as increased covariance between the visual and transmodal cortex, which is consistent with our Early adaptation results. Likewise, by the end of learning, when visual errors have been reduced to near baseline levels, the feedforward exchange of information from the visual to transmodal cortex would be expectantly reduced. This would presumably manifest as decreased covariance between the visual and transmodal cortex, which is also consistent with our Late adaptation results.

Another, albeit not mutually exclusive, possibility is that the pattern of manifold expansion-then-contraction of the visual cortex described above relates to learning-dependent changes in the top–down modulation of visual cortical activity by the transmodal cortex. For instance, during Early adaptation, when visual errors are large and numerous (and when learning rates are maximal), the attentional processing of visual errors is likely to be heightened and prioritized as compared to during Late adaptation, when errors tend to be much smaller in magnitude and when performance has more or less stabilized. Prior work has shown that the allocation of attentional resources during learning plays a critical role in successful sensorimotor adaptation (78–80) and, similarly, that the allocation of spatial attention during motor planning modulates neural activity in the visual cortex (88–90). Although the neural circuits by which the visual cortex is modulated during tasks involving motor learning and control remain poorly understood, such modulation likely involves top–down projections from higher-order brain areas in the association cortex (91, 92). Taken together, our visual cortex findings are likely to be explained, at least in part, by both bottom–up and top–down interactions between the transmodal and visual cortices.

In summary, here we applied recent dimensionality reduction approaches in order to describe the changing functional architecture of the cortex during sensorimotor learning. This approach enabled us to identify adaptation-related shifts in a low-dimensional connectivity structure that are driven by increasing integration between regions within sensorimotor and higher-order association networks, and later in adaptation, functional segregation of visual areas. These findings offer a unique perspective in our understanding of the cortical contributions to sensorimotor adaptation, which not only have important implications in contemporary theories of motor learning but also the role of the transmodal cortex in task-based performance.

Materials and Methods

40 right-handed individuals (13 males) between the ages of 18 and 35 ($M = 22.5$, $SD = 4.51$) participated in the study. Data from eight participants were excluded due to head motion in the scanner or missing scans. Participants' written, informed consent was obtained before commencement of the experimental protocol. The Queen's University Research Ethics Board approved the study, and it was conducted in accordance with the principles outlined in the Canadian Tri-Council Policy Statement on Ethical Conduct for Research Involving Humans and the principles of the Declaration of Helsinki (1964).

We used a well-established motor learning paradigm, the visuomotor rotation task (55), to probe sensorimotor adaptation. This task consisted of launching a cursor from an initial center position to a cued target at one of eight possible encircling locations, which was performed by applying a directional force onto an MRI-compatible force sensor. During a continuous fMRI scan, a total of 440 trials were completed, which included 120 trials with no cursor rotation (i.e., aligned to the force direction) and 320 subsequent trials with a 45° cursor rotation. For each participant, region time series were extracted by taking the mean blood oxygenation level-dependent (BOLD) activity of each 998 brain regions according to the Schaefer 1000 parcellation (56), which were then spliced into three task epochs: Baseline (120 trials prior to cursor rotation), Early adaptation (120 trials immediately following cursor rotation), and Late adaptation (the final 120 trials with cursor rotation). We generated centered functional connectivity matrices for each epoch, which were then transformed to cosine similarity affinity matrices after undergoing row-wise proportional thresholding (i.e., top 10% connections each row; *SI Appendix, Materials and Methods*). We applied PCA on each affinity matrix to construct connectivity manifolds (26, 62, 63) for each participant and task epoch, which were aligned to a group-average template Baseline manifold using Procrustes alignment. To assess adaptation-related changes in manifold structure, we computed each region's manifold eccentricity (52, 53, 69), and identified region-wise differences in eccentricity across task epochs using repeated-measures ANOVAs, as well as post hoc pairwise contrasts using paired *t*-tests. To examine the changes in whole-brain connectivity that underlie changes in manifold eccentricity, we performed seed connectivity contrasts of four exemplar regions that demonstrate representative effects. Additionally, we related individual differences in manifold structure during Early adaptation with differences in performance. We correlated participants' median angular error with a) the eccentricity of each region and b) the mean eccentricity of entire functional networks during Early adaptation. For complete methods, refer to *SI Appendix, Materials and Methods*.

Data, Materials, and Software Availability. Neuroimaging data have been deposited in Visuomotor rotation adaptation experiment (10.18112/openneuro.ds004021.v1.0.0). Analysis code is available at https://github.com/danjgale/adaptation-manifolds.

ACKNOWLEDGMENTS. This work was supported by operating grants from the Canadian Institutes of Health Research (CIHR) awarded to J.P.G. (MOP126158). J.P.G. was also supported by an NSERC Discovery Grant, as well as funding from the Canadian Foundation for Innovation. D.J.G. was supported by a Natural Sciences and Engineering Research Council (NSERC) graduate award, and portions of this work were developed from the third chapter of D.J.G.'s Ph.D. thesis. We thank Martin York, Sean Hickman, Don O'Brien, and Michael Lewis for technical assistance.

Author affiliations: [a]Centre for Neuroscience, Queen's University, Kingston, ON K7L 3N6, Canada; [b]Department of Psychology, Queen's University, Kingston, ON K7L 3N6, Canada; [c]Montréal Neurological Institute, McGill University, Montréal, QC H3A 0G4, Canada; and [d]Department of Biomedical and Molecular Sciences, Queen's University, Kingston, ON K7L 3N6, Canada

1. J. M. Pearson, S. R. Heilbronner, D. L. Barack, B. Y. Hayden, M. L. Platt, Posterior cingulate cortex: Adapting behavior to a changing world. *Trends Cogn. Sci.* **15**, 143–151 (2011).
2. J. Gottlieb, P. Y. Oudeyer, Towards a neuroscience of active sampling and curiosity. *Nat. Rev. Neurosci.* **19**, 758–770 (2018).
3. F. Arce, I. Novick, Y. Mandelblat-Cerf, E. Vaadia, Neuronal correlates of memory formation in motor cortex after adaptation to force field. *J. Neurosci.* **30**, 9189–9198 (2010).
4. Y. Mandelblat-Cerf, R. Paz, E. Vaadia, Trial-to-trial variability of single cells in motor cortices is dynamically modified during visuomotor adaptation. *J. Neurosci.* **29**, 15053–15062 (2009).

5. Y. Mandelblat-Cerf *et al*., The neuronal basis of long-term sensorimotor learning. *J. Neurosci.* **31**, 300–313 (2011).
6. Y. W. Tseng, J. Diedrichsen, J. W. Krakauer, R. Shadmehr, A. J. Bastian, Sensory prediction errors drive cerebellum-dependent adaptation of reaching. *J. Neurophysiol.* **98**, 54–62 (2007).
7. R. Shadmehr, H. H. Holcomb, Neural correlates of motor memory consolidation. *Science* **277**, 821–825 (1997).
8. J. Diedrichsen, Y. Hashambhoy, T. Rane, R. Shadmehr, Neural correlates of reach errors. *J. Neurosci.* **25**, 9919–9931 (2005).
9. R. M. Hardwick, C. Rottschy, R. C. Miall, S. B. Eickhoff, A quantitative meta-analysis and review of motor learning in the human brain. *Neuroimage* **67**, 283–297 (2013).
10. D. M. Wolpert, Z. Ghahramani, M. I. Jordan, An internal model for sensorimotor integration. *Science* **269**, 1880–1882 (1995).
11. J. Schlerf, R. B. Ivry, J. Diedrichsen, Encoding of sensory prediction errors in the human cerebellum. *J. Neurosci.* **32**, 4913–4922 (2012).
12. R. Shadmehr, J. W. Krakauer, A computational neuroanatomy for motor control. *Exp. Brain Res.* **185**, 359–381 (2008).
13. R. Shadmehr, M. A. Smith, J. W. Krakauer, Error correction, sensory prediction, and adaptation in motor control. *Annu. Rev. Neurosci.* **33**, 89–108 (2010).
14. J. A. Taylor, N. M. Klemfuss, R. B. Ivry, An explicit strategy prevails when the cerebellum fails to compute movement errors. *Cerebellum* **9**, 580–586 (2010).
15. J. A. Taylor, R. B. Ivry, Cerebellar and prefrontal cortex contributions to adaptation, strategies, and reinforcement learning. *Prog. Brain Res.* **210**, 217–253 (2014).
16. S. D. McDougle, R. B. Ivry, J. A. Taylor, Taking aim at the cognitive side of learning in sensorimotor adaptation tasks. *Trends Cogn. Sci.* **20**, 535–544 (2016).
17. P. Mazzoni, J. W. Krakauer, An implicit plan overrides an explicit strategy during visuomotor adaptation. *J. Neurosci.* **26**, 3642–3645 (2006).
18. J. A. Taylor, J. W. Krakauer, R. B. Ivry, Explicit and implicit contributions to learning in a sensorimotor adaptation task. *J. Neurosci.* **34**, 3023–3032 (2014).
19. A. J. de Brouwer, M. Albaghdadi, J. R. Flanagan, J. P. Gallivan, Using gaze behavior to parcellate the explicit and implicit contributions to visuomotor learning. *J. Neurophysiol.* **120**, 1602–1615 (2018).
20. J. Fernandez-Ruiz, W. Wong, I. T. Armstrong, J. R. Flanagan, Relation between reaction time and reach errors during visuomotor adaptation. *Behav. Brain Res.* **219**, 8–14 (2011).
21. A. J. de Brouwer *et al*., Human variation in Error-Based and reinforcement motor learning is associated with entorhinal volume. *Cereb. Cortex* **32**, 3423–3440 (2022).
22. J. A. Anguera, C. A. Russell, D. C. Noll, R. D. Seidler, Neural correlates associated with intermanual transfer of sensorimotor adaptation. *Brain Res.* **1185**, 136–151 (2007).
23. J. A. Anguera, P. A. Reuter-Lorenz, D. T. Willingham, R. D. Seidler, Contributions of spatial working memory to visuomotor learning. *J. Cogn. Neurosci.* **22**, 1917–1930 (2010).
24. J. Smallwood *et al*., The default mode network in cognition: A topographical perspective. *Nat. Rev. Neurosci.* **22**, 503–513 (2021).
25. M. M. Mesulam, From sensation to cognition. *Brain* **121** (Pt 6), 1013–1052 (1998).
26. D. S. Margulies *et al*., Situating the default-mode network along a principal gradient of macroscale cortical organization. *Proc. Natl. Acad. Sci. U. S. A.* **113**, 12574–12579 (2016).
27. J. R. Andrews-Hanna, J. S. Reidler, J. Sepulcre, R. Poulin, R. L. Buckner, Functional-anatomic fractionation of the brain's default network. *Neuron* **65**, 550–562 (2010).
28. K. Christoff, A. M. Gordon, J. Smallwood, R. Smith, J. W. Schooler, Experience sampling during fmri reveals default network and executive system contributions to mind wandering. *Proc. Natl. Acad. Sci. U. S. A.* **106**, 8719–8724 (2009).
29. D. Konu *et al*., A role for the ventromedial prefrontal cortex in self-generated episodic social cognition. *Neuroimage* **218**, 116977 (2020).
30. R. L. Buckner, J. R. Andrews-Hanna, D. L. Schacter, The brain's default network: Anatomy, function, and relevance to disease. *Ann. N.Y. Acad. Sci.* **1124**, 1–38 (2008).
31. M. E. Raichle, The brain's default mode network. *Annu. Rev. Neurosci.* **38**, 433–447 (2015).
32. J. M. Pearson, B. Y. Hayden, S. Raghavachari, M. L. Platt, Neurons in posterior cingulate cortex signal exploratory decisions in a dynamic multioption choice task. *Curr. Biol.* **19**, 1532–1537 (2009).
33. P. H. Rudebeck, E. A. Murray, Dissociable effects of subtotal lesions within the macaque orbital prefrontal cortex on reward-guided behavior. *J. Neurosci.* **31**, 10569–10578 (2011).
34. J. M. Pearson, S. R. Heilbronner, D. L. Barack, B. Y. Hayden, M. L. Platt, Posterior cingulate cortex: Adapting behavior to a changing world. *Trends Cogn. Sci.* **15**, 143–151 (2011).
35. M. Sormaz *et al*., Default mode network can support the level of detail in experience during active task states. *Proc. Natl. Acad. Sci. U.S.A.* **115**, 9318–9323 (2018).
36. D. Vatansever, D. K. Menon, E. A. Stamatakis, Default mode contributions to automated information processing. *Proc. Natl. Acad. Sci. U.S.A.* **114**, 12821–12826 (2017).
37. C. Murphy *et al*., Distant from input: Evidence of regions within the default mode network supporting perceptually-decoupled and conceptually-guided cognition. *Neuroimage* **171**, 393–401 (2018).
38. C. Murphy *et al*., Modes of operation: A topographic neural gradient supporting stimulus dependent and independent cognition. *Neuroimage* **186**, 487–496 (2019).
39. D. Vatansever, D. K. Menon, A. E. Manktelow, B. J. Sahakian, E. A. Stamatakis, Default mode dynamics for global functional integration. *J. Neurosci.* **35**, 15254–15262 (2015).
40. A. Turnbull *et al*., The ebb and flow of attention: Between-subject variation in intrinsic connectivity and cognition associated with the dynamics of ongoing experience. *Neuroimage* **185**, 286–299 (2019).
41. K. V. Shenoy, M. Sahani, M. M. Churchland, Cortical control of arm movements: A dynamical systems perspective. *Annu. Rev. Neurosci.* **36**, 337–359 (2013).
42. J. A. Gallego, M. G. Perich, L. E. Miller, S. A. Solla, Neural manifolds for the control of movement. *Neuron* **94**, 978–984 (2017).
43. J. P. Cunningham, M. Y. Byron, Dimensionality reduction for large-scale neural recordings. *Nat. Neurosci.* **17**, 1500–1509 (2014).
44. D. S. Bassett, O. Sporns, Network neuroscience. *Nat. Neurosci.* **20**, 353–364 (2017).
45. J. M. Shine *et al*., Human cognition involves the dynamic integration of neural activity and neuromodulatory systems. *Nat. Neurosci.* **22**, 289–296 (2019).
46. C. Paquola *et al*., Shifts in myeloarchitecture characterise adolescent development of cortical gradients. *Elife* **8**, e50482 (2019).
47. C. Paquola *et al*., Microstructural and functional gradients are increasingly dissociated in transmodal cortices. *PLoS Biol.* **17**, e3000284 (2019).
48. S. L. Valk *et al*., Shaping brain structure: Genetic and phylogenetic axes of macroscale organization of cortical thickness. *Sci. Adv.* **6**, eabb3417 (2020).
49. S. J. Hong *et al*., Atypical functional connectome hierarchy in autism. *Nat. Commun.* **10**, 1022 (2019).
50. M. Xia *et al*., Connectome gradient dysfunction in major depression and its association with gene expression profiles and treatment outcomes. *Mol. Psychiatry* **27**, 1384–1393 (2022).
51. R. Vos *et al*., Structural connectivity gradients of the temporal lobe serve as multiscale axes of brain organization and cortical evolution. *Cereb. Cortex* **31**, 5151–5164 (2021).
52. R. A. I. Bethlehem *et al*., Dispersion of functional gradients across the adult lifespan. *Neuroimage* **222**, 117299 (2020).
53. B. Y. Park *et al*., An expanding manifold in transmodal regions characterizes adolescent reconfiguration of structural connectome organization. *Elife* **10** (2021).
54. R. Setton *et al*., Age differences in the functional architecture of the human brain. *Cereb. Cortex* (2022).
55. J. W. Krakauer, Motor learning and consolidation: The case of visuomotor rotation. *Adv. Exp. Med. Biol.* **629**, 405–421 (2009).
56. A. Schaefer *et al*., Local-Global parcellation of the human cerebral cortex from intrinsic functional connectivity MRI. *Cereb. Cortex* **28**, 3095–3114 (2018).
57. C. Gratton *et al*., Functional brain networks are dominated by stable group and individual factors, not cognitive or daily variation. *Neuron* **98**, 439–452.e5 (2018).
58. Q. Zhao, D. Kwon, K. M. Pohl, A riemannian framework for longitudinal analysis of Resting-State functional connectivity. *Med. Image Comput. Comput. Assist. Interv.* **11072**, 145–153 (2018).
59. C. N. Areshenkoff *et al*., Muting, not fragmentation, of functional brain networks under general anesthesia. *Neuroimage* **231**, 117830 (2021).
60. C. Areshenkoff *et al*., Neural excursions from manifold structure explain patterns of learning during human sensorimotor adaptation. *Elife* **11**, e74591 (2022).
61. L. McInnes, J. Healy, J. Melville, Umap: Uniform manifold approximation and projection for dimension reduction. arXiv:1802.03426 arXiv preprint (2010).
62. R. Vos *et al*., BrainSpace: A toolbox for the analysis of macroscale gradients in neuroimaging and connectomics datasets. *Commun. Biol.* **3**, 103 (2020).
63. S. J. Hong *et al*., Toward a connectivity gradient-based framework for reproducible biomarker discovery. *Neuroimage* **223**, 117322 (2020).
64. B. T. T. Yeo *et al*., The organization of the human cerebral cortex estimated by intrinsic functional connectivity. *J. Neurophysiol.* **106**, 1125–1165 (2011).
65. J. M. Huntenburg, P. L. Bazin, D. S. Margulies, Large-Scale gradients in human cortical organization. *Trends Cogn. Sci.* **22**, 21–31 (2018).
66. J. P. Gallivan, D. A. McLean, K. F. Valyear, C. E. Pettypiece, J. C. Culham, Decoding action intentions from preparatory brain activity in human parieto-frontal networks. *J. Neurosci.* **31**, 9599–9610 (2011).
67. J. P. Gallivan, D. A. McLean, J. R. Flanagan, J. C. Culham, Where one hand meets the other: Limb-specific and action-dependent movement plans decoded from preparatory Signals in single human frontoparietal brain areas. *J. Neurosci.* **33**, 1991–2008 (2013).
68. J. P. Gallivan, J. C. Culham, Neural coding within human brain areas involved in actions. *Curr. Opin. Neurobiol.* **33**, 141–149 (2015).
69. B. Y. Park *et al*., Inter-individual body mass variations relate to fractionated functional brain hierarchies. *Commun. Biol.* **4**, 735 (2021).
70. M. Corbetta, G. L. Shulman, Control of goal-directed and stimulus-driven attention in the brain. *Nat. Rev. Neurosci.* **3**, 201–215 (2002).
71. S. V. Astafiev *et al*., Functional organization of human intraparietal and frontal cortex for attending, looking, and pointing. *J. Neurosci.* **23**, 4689–4699 (2003).
72. S. M. Szczepanski, M. A. Pinsk, M. M. Douglas, S. Kastner, Y. B. Saalmann, Functional and structural architecture of the human dorsal frontoparietal attention network. *Proc. Natl. Acad. Sci. U. S. A.* **110**, 15806–15811 (2013).
73. J. W. Krakauer, A. M. Hadjiosif, J. Xu, A. L. Wong, A. M. Haith, Motor learning. *Compr. Physiol.* **9**, 613–663 (2019).
74. J. W. Krakauer *et al*., Differential cortical and subcortical activations in learning rotations and gains for reaching: A PET study. *J. Neurophysiol.* **91**, 924–933 (2004).
75. B. Aben, C Buc Calderon, E Van den Bussche, T Verguts, Cognitive effort modulates connectivity between dorsal anterior cingulate cortex and Task-Relevant cortical areas. *J. Neurosci.* **40**, 3838–3848 (2020).
76. P. Bédard, J. H. Song, Attention modulates generalization of visuomotor adaptation. *J. Vis.* **13**, 12–12 (2013).
77. N. M. Drummond, E. K. Cressman, A. N. Carlsen, Inhibition of motor-related activation during a simple reaction time task requiring visuomotor mental rotation. *Behav. Neurosc.* **129**, 160 (2015).
78. J. A. Taylor, K. A. Thoroughman, Divided attention impairs human motor adaptation but not feedback control. *J. Neurophysiol.* **98**, 317–326 (2007).
79. J. A. Taylor, K. A. Thoroughman, Motor adaptation scaled by the difficulty of a secondary cognitive task. *PLoS One* **3**, e2485 (2008).
80. J. H. Song, The role of attention in motor control and learning. *Curr. Opin. Psych.* **29**, 261–265 (2019).
81. D. L. Schacter, D. R. Addis, The cognitive neuroscience of constructive memory: Remembering the past and imagining the future. *Philos. Trans. R. Soc. B: Biol. Sci.* **362**, 773–786 (2007).
82. J. R. Binder, R. H. Desai, W. W. Graves, L. L. Conant, Where is the semantic system? a critical review and meta-analysis of 120 functional neuroimaging studies. *Cereb. Cortex* **19**, 2767–2796 (2009).
83. K. Krieger-Redwood *et al*., Down but not out in posterior cingulate cortex: Deactivation yet functional coupling with prefrontal cortex during demanding semantic cognition. *Neuroimage* **141**, 366–377 (2016).
84. D. J. Herzfeld, P. A. Vaswani, M. K. Marko, R. Shadmehr, A memory of errors in sensorimotor learning. *Science* **345**, 1349–1353 (2014).

85. M. Konishi, D. G. McLaren, H. Engen, J. Smallwood, Shaped by the past: The default mode network supports cognition that is independent of immediate perceptual input. *PloS one* **10**, e0132209 (2015).
86. J. R. Morehead, S. E. Qasim, M. J. Crossley, R. Ivry, Savings upon Re-Aiming in visuomotor adaptation. *J. Neuroscience* **35**, 14386–14396 (2015).
87. K. M. Bond, J. A. Taylor, Flexible explicit but rigid implicit learning in a visuomotor adaptation task. *J. Neurophysiol.* **113**, 3836–3849 (2015).
88. C. S. Chapman, J. P. Gallivan, J. C. Culham, M. A. Goodale, Mental blocks: Fmri reveals top-down modulation of early visual cortex when obstacles interfere with grasp planning. *Neuropsychologia* **49**, 1703–1717 (2011).
89. T. P. Gutteling *et al*., Action preparation shapes processing in early visual cortex. *J. Neurosci.* **35**, 6472–6480 (2015).
90. J. P. Gallivan, C. S. Chapman, D. J. Gale, J. R. Flanagan, J. C. Culham, Selective modulation of early visual cortical activity by movement intention. *Cereb. Cortex* **29**, 4662–4678 (2019).
91. C. D. Gilbert, W. Li, Top-down influences on visual processing. *Nat. Rev. Neurosci.* **14**, 350–363 (2013).
92. L. Muckli, L. S. Petro, Network interactions: Non-geniculate input to v1. *Curr. Opin. Neurobiol.* **23**, 195–201 (2013).